

A plasmon enhanced attosecond extreme ultraviolet source

Mattia Lupetti^a, Matthias F. Kling^{b,c}, and Armin Scrinzi^{a*}

^a*Ludwig Maximilians Universität, Munich, Germany*

^b*Max-Planck-Institut für Quantenoptik, Garching, Germany*

^c*J.R. Macdonald Laboratory, Kansas State University, Manhattan, USA*

(Dated: November 6, 2018)

Abstract

A compact high repetition rate attosecond light source based on a standard laser oscillator combined with plasmonic enhancement is presented. At repetition rates of tens of MHz, we predict focusable pulses with durations of $\lesssim 300$ attoseconds, and collimation angles $\lesssim 5^\circ$. Attosecond pulse parameters are robust with respect variations of driver pulse focus and duration.

High harmonic sources with controlled attosecond ($1 \text{ as} = 10^{-18} \text{ s}$) time structure allow the observation of electronic dynamics on the natural time-scale of valence electrons. A range of recently developed techniques for ultrafast spectroscopy rely on such sources, for example, attosecond streaking of photo-emission from atoms [1, 2], and solid surfaces [3], as well as attosecond transient absorption spectroscopy [4].

The attosecond pulse sources used in present experiments are all based on high harmonic emission from gases. An extremely non-linear conversion process — ingeniously described by the classical three-step re-collision model [5, 6] — imprints the time-structure of the driving laser pulse onto the harmonic radiation. Non-linearity sharpens the original sine-like driver electric field to produce bursts of high frequency radiation which may be as short as 67 attoseconds [7]. The bursts are time-delayed relative to the maxima of the driver field by ~ 0.2 driver optical cycles, i.e. emission occurs near the *nodes* of the driver field. The time-locking of the attosecond pulse to the driver is exploited for precision time-delay experiments with time resolutions down to $\sim 10 \text{ as}$.

Other than pulse duration, key parameters of the sources are photon energy, pulse separation, peak and average intensity, and for certain applications [8], focal spot size. Maximal photon energies of high gas harmonics depend on driver pulse intensity as $\sim I_p + 3.2 U_p$, where I_p is the ionization potential of the gas and U_p is the driver ponderomotive potential. This dependency is a direct consequence of the re-collision mechanism for their generation. For photon-energies $\gtrsim 40 \text{ eV}$ with pulses at the Ti:sapphire wavelength of 800 nm one needs intensities $\gtrsim 10^{14} \text{ W/cm}^2$. At driver pulse durations $\sim 20 \text{ fs}$ a short “train” of attosecond pulses is generated, i.e. a sequence of a few pulses separated from each other by half the driver optical period, as each half-cycle near the peak intensity creates its own burst. While trains of attosecond pulses are comparatively easy to generate, using them for time-resolving processes that extend over more than half an optical period ($\sim 1.3 \text{ fs}$) is difficult and requires deconvolution of the overlapping signals from neighboring pulses.

Isolated single attosecond pulses are generated by using extremely short driver pulses where only one optical cycle is strong enough to generate high harmonics at the relevant photon energies [9]. Alternatively to short pulses, one can also manipulate polarization on the time scale of a single optical cycle in order to suppress high harmonic generation for all but one field peak [10]. With this mechanism, time-separation is given by the separation of subsequent driver pulses rather than by the optical half-cycle. These techniques are

experimentally complex. While laser oscillators delivering pulses as short as 4 fs FWHM at 80 MHz repetition rate are available [11], amplification to $\gtrsim 10^{14} W/cm^2$ brings the repetition rate down into the kilohertz regime.

In a recent paper [12] plasmonic excitation in a cone-shaped silver funnel was proposed to replace the laser amplification stages and directly use the high repetition rate oscillator for locally generating the intensities needed for high harmonics. Significant field enhancement was theoretically predicted and extreme ultraviolet (XUV) radiation was detected experimentally. A follow-up theoretical study systematically investigated the dependence of the plasmonic field on funnel geometry and drive pulse parameters [13]. The fields were found to produce attosecond time structure in the response of an isolated atom.

In the present work we investigate, whether the harmonic radiation is emitted from the funnel in the form of a usable beam and whether the time-structure is maintained in the macroscopic response. We find that emission from the narrow end of the funnel is severely diffracted rendering it very hard to use in experiments. In contrast, in the reverse direction from the large opening of the funnel a well-collimated beam with single attosecond pulse structure is emitted. This “plasmon enhanced attosecond XUV source” (PEAX) is compared to standard attosecond gas harmonic sources in terms of beam quality and yield. Our analysis is based on solving the three-dimensional Maxwell equations for propagation of driver, plasmon, and harmonic fields, and solving the atomic time-dependent Schrödinger equation for the microscopic high harmonic response.

Similar as in reference [12] we chose for our simulations a $9\mu m$ long silver cone with elliptic cross-section and opening angles of 14 and 3.5 degrees along the major (x -) and minor (y -)axis of the ellipse, respectively. We assume a 5 fs FWHM Gaussian driver pulse at wavelength $\lambda_0 = 800 nm$, beam waist $w_0 = 2.5\mu m$, and focused intensity $I_0 \approx 4 \times 10^{11} W/cm^2$. The focal spot is placed at the larger opening of the cone (see Figure 1). Variations of the focus position by $\pm 1\mu m$ cause intensity changes of less than 5% in peak plasmon intensity. For solving Maxwell’s equations we used the finite difference time-domain open source code MEEP [14]. For algorithmic reasons, dielectric functions in MEEP must have Lorentzian shape, which poorly reproduces the known dielectric response of silver at photon energies around 60 eV. Care was taken to accurately fit the imaginary part of the response (Fig. 2). We found that the real part of the dielectric response has little influence on the results: with the two vastly different responses shown in Fig. 2 intensity and time-

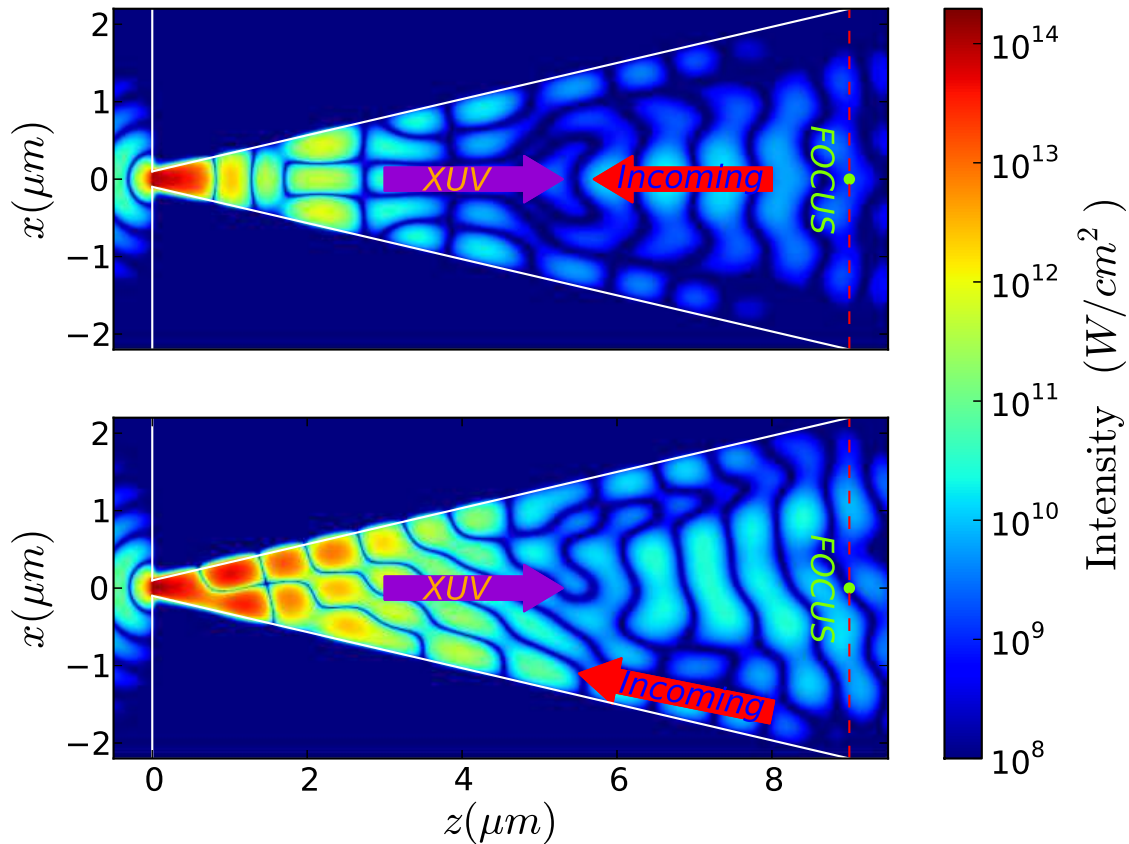


FIG. 1. (color online) Intensity distribution in the silver cone in the xz -plane at peak plasmon field of $2 \times 10^{14} W/cm^2$. Normal (upper panel) and oblique incidence (lower panel). Polarization is in y -direction perpendicular to the plane. Oblique incidence angle is 7 degrees in the zx -plane parallel to the inner cone surface. In both cases, the harmonic beam is emitted in the direction of the cone axis.

structure of the final harmonic signal change by less than 15%.

As observed in Ref. [12], the elliptic cross-section of the cone improves the plasmonic enhancement of the evanescent wave. With strong eccentricity of $\epsilon = 0.25$ we find an enhancement of ~ 500 over the peak intensity of the incident driver field. With $\epsilon = 0.5$ used in Ref. [12] the enhancement reduced by about a factor 3. A similar dependence on ellipticity was reported in [13], where pulse durations between 4 and 10 fs were investigated. Note that peak field is reached at the surface and therefore surface roughness will introduce modifications of the exact maxima. However, harmonics are produced in volumes of the

scale of the evanescent wave, which are less subjected to such sub-wavelength modifications. Optimizing the cone geometry allows for even weaker driver pulses. Note however, that ultimately the field inside the cone is limited by damage to the silver surface. Fortunately, in [12] it was found that silver can support much higher fields than expected, likely due to the extreme shortness of the pulses [15].

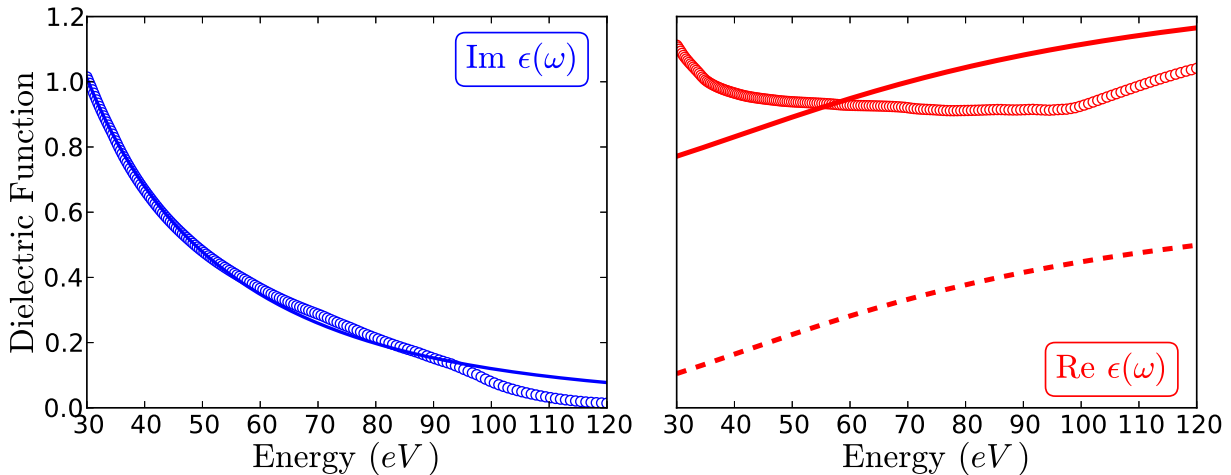


FIG. 2. (color online) Dielectric functions used for the simulation of high harmonic propagation. Imaginary parts of the experimental values (left, blue circles) are well approximated by a Lorentzian shape (blue line), The fit (right, red line) of the experimental real values (circles) is comparatively poor. The deliberately bad fit (dashed line) was used for checking robustness of the simulation (see text).

For high harmonic propagation, the driver field was sampled with grid points separated by 2.5 nm , well below the characteristic wavelength of 800 nm of the driver plasmon in the cone and below the relevant harmonic wavelengths of $\sim 27 \text{ nm}$. The atomic responses were obtained by solving the time-dependent Schrödinger equation by the irECS method [16] using a single-electron model with the ionization potential of Argon. The harmonic yield drops rapidly with driver field intensity: from $2 \times 10^{14} \text{ W/cm}^2$ to $1 \times 10^{14} \text{ W/cm}^2$ the yield near the cutoff photon energy of $\sim 60 \text{ eV}$ drops by ~ 3 orders of magnitude. We therefore restricted the calculation of the responses to the volume $x \times y \times z \approx 240 \times 60 \times 500 \text{ nm}^3$, where driver intensity exceeded 10^{14} W/cm^2 .

Coupling of the driver into the cone and harmonic emission can be maintained over a range of incidence angles. Comparing to driver incidence on axis, plasmonic enhancement

drops by about a factor 4 at incidence angle 7 degrees around the polarization (y -) axis, parallel to the inner cone surface at the major axis. The smaller enhancement can be compensated by an increase in driver intensity.

At short wavelength, numerical propagation through the complete cone in three dimensions leads to an inappropriately large computational problem. However, the influence of the cone on the propagation of short wavelength radiation can be expected to be small. We tested this assumption in a wedge-shaped silver structure, where symmetry allows reduction to a two-dimensional problem. We found that guiding in the silver cone improves collimation of the beam compared to propagation in vacuum, but leaves the time structure largely unaffected. Numerical convergence of the propagation in vacuum was verified by direct numerical summation of the Liénard-Wiechert potentials of the individual atomic dipoles. Propagation from the end of the cone to large distances is given by Kirchhoff's diffraction integral.

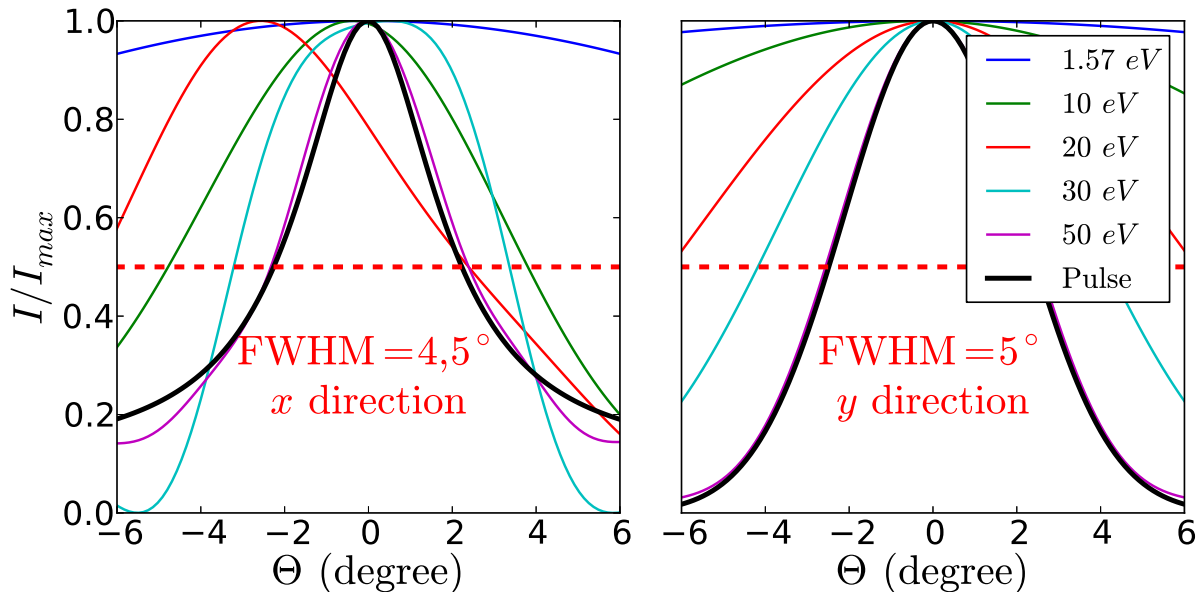


FIG. 3. (color online) Far field angular distribution at a range of photon energies. The asymmetry in the left panel (x -direction) is due to the oblique incidence. The right panel shows polarization- (y -) direction. Profiles are taken at 1 mm distance from the cone. The thick black lines show divergence for a pulse composed of all harmonics above 45 eV.

We compute the far field in the three-dimensional geometry from the Kirchhoff integral with the MEEP solution at $z = 2.5\mu m$. Figure 3 shows the angular distribution of harmonic

TABLE I. Harmonic beam characteristics for oblique incidence PEAX and a standard harmonic source using a Gaussian beam (see text for parameters). Yields and photon flux are integrated over the beam divergence angles.

	PEAX	Gauss
Photon energy ω_γ	45 eV	45 eV
Pulse duration Δt	300 as	250 as
Rep Rate	80 MHz	3 kHz
Yield per pulse	$6.7 \cdot 10^{-3} \gamma/\text{pulse}$	$3 \cdot 10^4 \gamma/\text{pulse}$
Photon flux	$5.4 \cdot 10^5 s^{-1}$	$9 \cdot 10^7 s^{-1}$
Beam divergence	5°	1°
Active volume	$\sim 4 \times 10^{-3} (\mu m)^3$	$\sim 16 (\mu m)^3$

emission out of the wide side of the cone for a range of harmonic frequencies at oblique driver incidence. The incident intensity was adjusted such as to obtain a peak field in the cone of $2 \times 10^{14} W/cm^2$. The beam divergence decreases with increasing photon energy, where the divergence angle is defined by decrease to half the peak intensity. For on-axis incidence, similar results are obtained, when the incident intensity is adjusted to give the same peak plasmon intensity. The effect of the driver incidence angle on the emitted beam is small, as the plasmon peak field is dominated by the same single plasmon mode, irrespective of the exact incidence angle.

With its extension $\lesssim 500 nm$ the volume over which harmonics are generated remains below the driver wavelength. Over that distance, free electron dispersion does not affect phase matching of the harmonic with the dominant plasmon mode. Similarly, atomic dispersion is expected to remain small, and, where needed, may be controlled by choosing a target gas suitable for a given harmonic wavelength. Geometrically induced phase shifts are automatically included in the simulation. With negligible phase slip between driver and harmonic across the generation volume, harmonic intensities grow quadratically with the gas density.

The first column of Table I shows the parameters of the harmonic pulses obtained at gas pressure of 0.3 bar (density $7.8 \cdot 10^{18} cm^{-3}$), a value typically used for standard gas harmonics. Due to the rapid decay of the spectral intensity with harmonic energy, the central frequency

nearly coincides with the lower cutoff frequency of the harmonics. The PEAX harmonics above 45 eV form an isolated attosecond pulse. Pulse contrast is satisfactory with 85% of the energy in the central peak.

The harmonic pulse is emitted with a perfectly spherical wave front. At a distance of 1 mm and over its divergence angle of 5° , the deviation from spherical shape remains below 5% of the central pulse wavelength. This can be ascribed to the very small and well-defined “focal spot”, i.e. the single plasmonic mode where the high harmonics are generated. The clean wave front allows for focusing without compromising the time-structure. The attosecond pulse is emitted on the cone axis, while the reflected driver and lower harmonics are emitted into wider angles with a modulated intensity profile (cf. Fig. 3). This allows simple geometric separation of the incident driver pulse from the harmonic pulse. Remaining on-axis components of the reflected driver and low harmonics can be blocked by standard filters.

Emission through the narrow end of the cone is comparable in photon-flux, but beam divergence is 35° in y -direction, making it hard to focus for experimental use.

The data given is for a 5 fs driver pulse. A shorter, 4 fs driver bears no further advantage: harmonic pulse duration and divergence remain unchanged, but emitted intensity is reduced by about 20%. Similarly, normal incidence of the driver does not improve harmonic pulse parameters, but rather leads to a reduction of intensity because of the smaller active volume (cf. Fig. 1).

In the second column of Table I, the pulse parameters for a traditional harmonic source are listed. For the comparison a Gaussian beam with 4 fs FWHM pulse duration was used. We assumed a tight focus in a gas jet with peak intensity in focus equal to the peak plasmonic intensity of $2 \times 10^{14}\text{ W/cm}^2$ and a beam waist of $1\mu\text{m}$. At the Rayleigh length of $3.9\mu\text{m}$, the volume for producing high harmonics is by three orders of magnitude larger than in PEAX. At our specific parameters, PEAX shows slightly longer pulse duration and larger beam divergence. Note that PEAX beam divergence is overestimated due to the omission of large part of the funnel in harmonic propagation. At photon energies $\sim 45\text{ eV}$ and at the given gas pressure, the photon yield per shot is almost 7 orders of magnitude larger compared to PEAX. This ratio corresponds to a ratio of a bit more than 3 orders of magnitude in field strengths, which is consistent with the ratio of the active volumes of the two sources. Due to the low required intensity, driver pulses for PEAX can be directly drawn from a laser

oscillator at repetition rates near 100 MHz, reducing the ratio of photon-fluxes between the two sources to $\lesssim 500$. With the very small active volume in PEAX, gas density can be increased significantly before an optical thickness is reached where phase matching problems arise and coherence of the source deteriorates. Assuming tenfold pressure for the PEAX, photon flux could be boosted by 2 orders of magnitude, basically closing the gap to the traditional gas harmonic source. Another obvious extension of PEAX would be to use an array of many instead of a single cone. Only recently, geometries with multiple cones were realized experimentally [17]. In such an arrangement, interference between the emission from different cones could be utilized for phase-matching.

However, it must be said that volumes for coherent gas harmonic generation can be significantly larger than what was assumed in our example. With proper placement of the beam focus relative to the gas jet, phase matching can be maintained over about 1 mm propagation length at a beam cross section of a few hundred μm^2 , further increasing volumes by 3-5 orders of magnitude over our example. This may turn out to be a fundamental limitation for intensities from any plasmon enhanced harmonic source: the natural length scale of the high intensity spots in such sources is the driver wavelength, while much larger diameters and phase matching length can be realized in gas harmonic sources. The motivation for using PEAX therefore rather arises from other advantages, such as its sub-micrometer collimated attosecond XUV beam, which may be used for spatio-time-resolved surface spectroscopy [8] and the high repetition rates that reduce space charge effects on the target. In principle, with the high repetition rate and possibly few-cycle pulses in the 45 eV (~ 27 nm wavelength) regime, frequency combs could be pushed to new parameter regimes. As plasmonic fields may vary over very spatial ranges non-dipole modifications of the atom-field interactions are introduced that may be exploited, e.g., for further reduction of pulse duration and for higher photon energies [18].

Technically, the PEAX appears simple as no strong few-cycle pulses are required. The mechanism is robust with respect to small variations in driver pulse focusing and duration. The weak dependence on incidence angles allows geometrical separation of the driver pulse from the attosecond pulse. Without the need for short pulse amplification and with its high repetition rate, PEAX is an attractive alternative source that may become accessible also outside specialized short pulse laboratories.

We acknowledge support by the DFG, by the excellence cluster "Munich Center for Ad-

vanced Photonics (MAP)”, and by the Austrian Science Foundation project ViCoM (F41). M. L. is a fellow of the IMPRS “Advanced Photon Science”. M.F.K. acknowledges support by the U.S. Department of Energy under de-sc0008146, the BMBF via PhoNa, and the DFG via Kl-1439/4 and Kl-1439/5. We are grateful for discussions with V. Yakovlev.

* mattia.lupetti@physik.uni-muenchen.de; armin.scrinzi@lmu.de

- [1] M. Drescher, *et al.* Nature **419**, 803 (2002).
- [2] T. Remetter, *et al.*, Nature Physics **2**, 323 (2006).
- [3] A. L. Cavalieri, *et al.*, Nature **449**, 1029 (2007).
- [4] E. Goulielmakis, *et al.*, Nature **466**, 739 (2010).
- [5] P. B. Corkum, Phys. Rev. Lett. **71**, 1994 (1993).
- [6] K. C. Kulander, K. J. Schafer, and J. L. Krause, Proceedings of the Workshop, Super Intense Laser Atom Physics (SILAP) III, edited by B. Piraux (Plenum, New York) (1993).
- [7] K. Zhao, *et al.*, Opt. Lett. **37**, 3891 (2012).
- [8] M. I. Stockman, M. F. Kling, U. Kleineberg, and F. Krausz, Nature Photonics **1**, 539 (2007).
- [9] A. Baltuška, *et al.*, Nature **421**, 611 (2003).
- [10] I. Sola, *et al.*, Nature Physics **2**, 319 (2006), ISSN 1745-2473.
- [11] S. Rausch, *et al.*, Optics Express **16**, 9739 (2008), ISSN 1094-4087.
- [12] I.-Y. Park, *et al.*, Nature Photonics **5**, 678 (2011).
- [13] J. Choi, *et al.*, New Journal of Physics **14**, 103038 (2012).
- [14] A. F. Oskooi, *et al.*, Comp. Phys. Comm. **181**, 687 (2010).
- [15] A. Plech, *et al.*, Nature Physics **2**, 44 (2006).
- [16] A. Scrinzi, Phys. Rev. A **81**, 053845 (2010).
- [17] S. Kim, private communication, under review for Annalen der Physik (2012).
- [18] T. Shaaran, M. F. Ciappina, and M. Lewenstein, Phys. Rev. A **86**, 023408 (2012).